# Thrombomodulin is essential for maintaining quiescence in vascular endothelial cells

Hemant Giri[a], Sumith R. Panicker[a], Xiaofeng Cai[a], Indranil Biswas[a], Hartmut Weiler[b], and Alireza R. Rezaie[a,c,1]

[a]Cardiovascular Biology Research Program, Oklahoma Medical Research Foundation, Oklahoma City, OK 73104; [b]Blood Research Institute, Blood Center of Wisconsin, Milwaukee, WI 53226; and [c]Department of Biochemistry and Molecular Biology, University of Oklahoma Health Sciences Center, Oklahoma City, OK 73104

Edited by Barry S. Coller, The Rockefeller University, New York, NY, and approved February 8, 2021 (received for review October 31, 2020)

**Thrombomodulin (TM) is a thrombin receptor on endothelial cells that is involved in promoting activation of the anticoagulant protein C pathway during blood coagulation. TM also exerts protective anti-inflammatory properties through a poorly understood mechanism. In this study, we investigated the importance of TM signaling to cellular functions by deleting it from endothelial cells by CRISPR-Cas9 technology and analyzed the resultant phenotype of TM-deficient ($TM^{-/-}$) cells. Deficiency of TM in endothelial cells resulted in increased basal permeability and hyperpermeability when stimulated by thrombin and TNF-α. The loss of the basal barrier permeability function was accompanied by increased tyrosine phosphorylation of VE-cadherin and reduced polymerization of F-actin filaments at cellular junctions. A significant increase in basal NF-κB signaling and expression of inflammatory cell adhesion molecules was observed in $TM^{-/-}$ cells that resulted in enhanced adhesion of leukocytes to $TM^{-/-}$ cells in flow chamber experiments. There was also a marked increase in expression, storage, and release of the von Willebrand factor (VWF) and decreased storage and release of angiopoietin-2 in $TM^{-/-}$ cells. In a flow chamber assay, isolated platelets adhered to $TM^{-/-}$ cells, forming characteristic VWF–platelet strings. Increased VWF levels and inflammatory foci were also observed in the lungs of tamoxifen-treated ERcre-$TM^{f/f}$ mice. Reexpression of the TM construct in $TM^{-/-}$ cells, but not treatment with soluble TM, normalized the cellular phenotype. Based on these results, we postulate cell-bound TM endows a quiescent cellular phenotype by tightly regulating expression of procoagulant, proinflammatory, and angiogenic molecules in vascular endothelial cells.**

thrombomodulin | inflammation | CRISPR-Cas9 | VWF | PAR1

Thrombomodulin (TM) is a high-affinity receptor for thrombin involved in promoting the activation of protein C to activated protein C (APC) on endothelial cells (1). APC has both anticoagulant and cytoprotective activities (2). APC initiates its cytoprotective activity through endothelial protein C receptor (EPCR)-dependent activation of protease-activated receptor 1 (PAR1) on endothelial cells (3, 4). PAR1 signaling by APC inhibits activation of NF-κB and expression of cell adhesion molecules (CAMs) and other proinflammatory cytokines in vascular endothelial cells (4, 5). TM contains five distinct domains: an N-terminal lectin-like domain, followed by six epidermal growth factor (EGF)-like domains, a membrane proximal Ser/Thr-rich domain harboring chondroitin sulfate glycosaminoglycans, a single-pass transmembrane domain, and a cytoplasmic tail (6). In addition to its essential cofactor role for thrombin in protein C activation, TM is known to directly elicit potent anti-inflammatory signaling responses in endothelial cells through a poorly understood mechanism. Recent results have indicated the lectin-like domain of TM exhibits anti-inflammatory functions in both cellular and animal models (7), likely by binding to an unknown receptor on endothelial cells. Moreover, the lectin-like domain of TM harbors binding sites for high mobility group box 1 (HMGB1) and lipopolysaccharides, thereby likely sequestering and attenuating their proinflammatory signaling functions (8). TM-deficient mice exhibit a severe consumptive coagulopathy with increased lung vascular permeability and inflammation (9). Transgenic supplementation of APC in these mice has been shown to suppress thrombosis, but it has failed to reduce increased lung permeability and inflammation (9), implicating a direct cytoprotective role for TM that appears to be independent of its cofactor role in promoting protein C activation by thrombin.

Analysis of the signaling data of thrombin, which has been studied in human umbilical vein endothelial cells (HUVECs), has proven to be challenging due to several negatively charged residues of both TM and PAR1 competing for binding to the same basic exosite-1 of thrombin (10), both receptors thereby being capable of influencing the signaling and functional specificity of the protease. Moreover, other factors, including cell surface expression levels of these receptors, their relative affinity for exosite-1, and the concentration of thrombin, can influence the interpretation of the experimental results (5). Because of these inherent complexities, the physiological relevance of the signaling data in HUVECs has remained obscure. In this vein, a potent PAR1-dependent proinflammatory function for thrombin in HUVECs has been reported; however, when a low concentration of catalytically inactive protein C zymogen (protein C-S195A) was added to cultured HUVECs in order to occupy EPCR, the cleavage of PAR1 by thrombin has been shown to induce a cytoprotective response (11), suggesting that coreceptor

## Significance

We demonstrate that deletion of thrombomodulin (TM) from endothelial cells confers inflammatory phenotype to TM-deficient ($TM^{-/-}$) cells. This is based on the loss of integrity of VE-cadherin at cellular junctions, disrupted basal barrier permeability, and increased expression of cell adhesion molecules in $TM^{-/-}$ cells. Proinflammatory phenotype is rescued by reexpression of TM in $TM^{-/-}$ cells; however, soluble TM lacked this effect. Interestingly, instead of storage in Weibel–Palade bodies, VWF was secreted in $TM^{-/-}$ cells, thereby recruiting platelets to cell surfaces under flow conditions. Increased VWF and inflammatory foci were also observed in lungs of tamoxifen-treated ERcre-$TM^{f/f}$ mice. These results suggest cell-bound TM maintains a quiescent phenotype in vascular endothelial cells by regulating expression of procoagulant and proinflammatory molecules.

Author contributions: H.G., S.R.P., and A.R.R. designed research; H.G., S.R.P., X.C., and I.B. performed research; H.W. and A.R.R. contributed new reagents/analytic tools; H.G., S.R.P., X.C., I.B., and A.R.R. analyzed data; and A.R.R. wrote the paper.

The authors declare no competing interest.

This article is a PNAS Direct Submission.



[1]To whom correspondence may be addressed. Email: ray-rezaie@omrf.org.

This article contains supporting information online at https://www.pnas.org/lookup/suppl/doi:10.1073/pnas.2022248118/-/DCSupplemental.

Published March 8, 2021.

signaling by EPCR plays a key role in determining the specificity of PAR1 signaling by thrombin (12). To determine the contribution of TM to signaling by thrombin on HUVECs, we decided to delete the TM gene in transformed HUVECs (EA.hy926 cells) using the CRISPR-Cas9 technology and investigated the inflammatory phenotypes of $TM^{-/-}$ cells under basal and stimulated conditions. We discovered that the basal barrier permeability and expression of cell surface adhesion molecules in $TM^{-/-}$ cells were elevated. Moreover, $TM^{-/-}$ cells exhibited significant hyperactivity for thrombin and other proinflammatory stimuli. Interestingly, we found that expression and secretion levels of von Willebrand factor (VWF) in $TM^{-/-}$ cells were dramatically elevated. By contrast expression and secretion levels of angiopoietin-2 (Ang2) were markedly decreased in these cells. Increased basal VWF levels and inflammatory foci were also observed in the lungs of tamoxifen-treated ERcre-$TM^{f/f}$ thrombomodulin knockout (TM-KO) mice. Reexpression of a TM construct in $TM^{-/-}$ cells normalized the endothelial cell phenotype. Based on these results, we hypothesize that TM endows a quiescent phenotype for vascular endothelial cell by tightly regulating expression of procoagulant and proinflammatory molecules.

## Results

**Deficiency of TM Results in Increased Basal Cell Permeability and Hyperresponsiveness to Inflammatory Stimuli.** To study the importance of TM for modulation of endothelial cell signaling in response to thrombin and other proinflammatory stimuli, we deleted the TM gene in EA.hy926 endothelial cells using CRISPR-Cas9 technology (*SI Appendix*, Fig. S1 *A* and *B*). Immunofluorescence analysis revealed a loss of VE-cadherin and reduced polymerization of F-actin filaments at cell junctions under basal conditions in $TM^{-/-}$ cells (Fig. 1*A*). The loss of the junctional VE-cadherin was accompanied by its increased tyrosine phosphorylation at Tyr658 (Fig. 1 *B* and *C*). No changes were observed in the total level of VE-cadherin or the tight junction protein, ZO-1, in $TM^{-/-}$ cells (Fig. 1*B*). TM was found to be colocalized with VE-cadherin at cellular junctions in wild-type EA.hy926 cells (*SI Appendix*, Fig. S2*A*). Increased tyrosine phosphorylation of VE-cadherin is known to disrupt stable interactions among junctional proteins and actin filaments, thereby

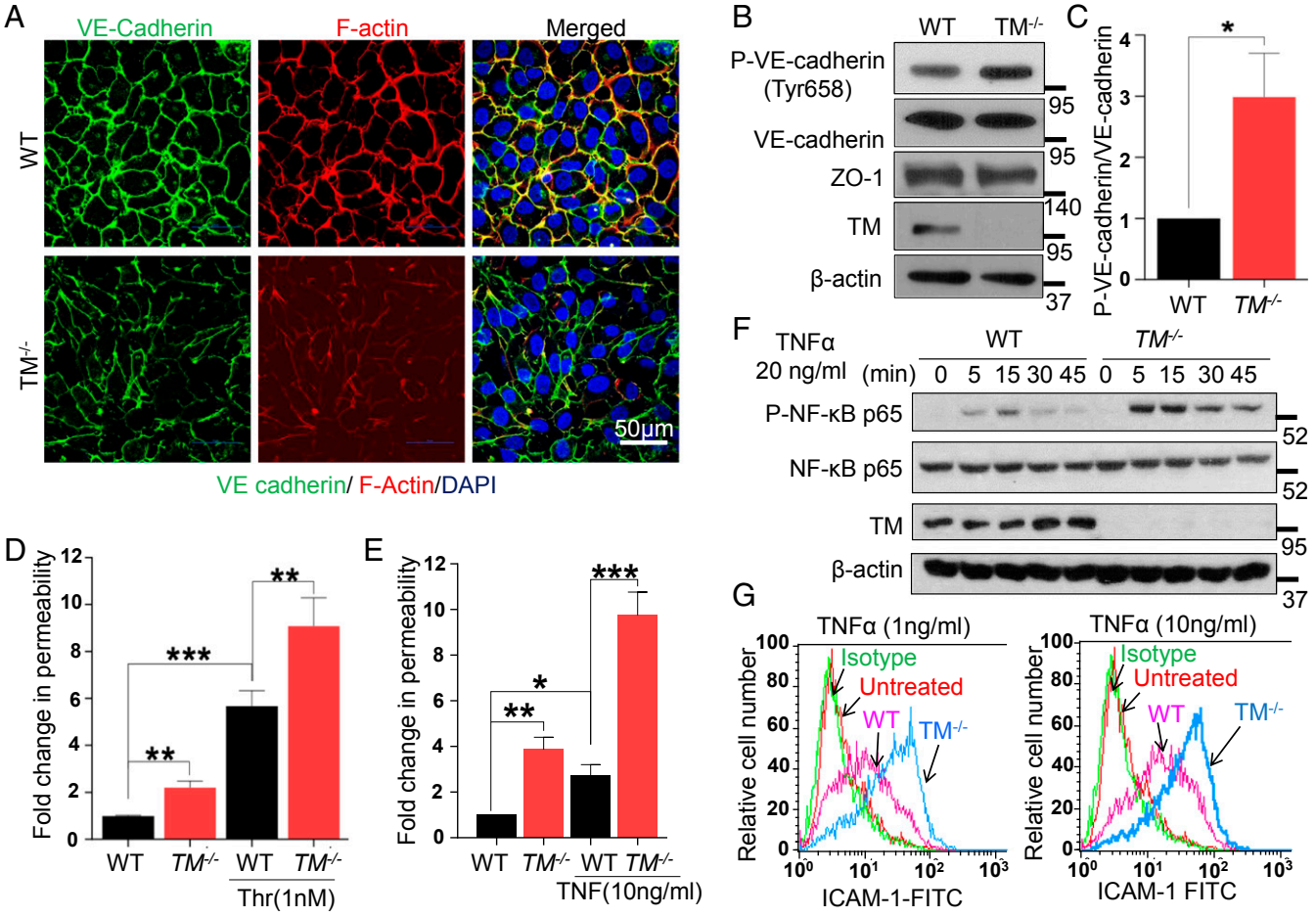


**Fig. 1.** Deficiency of TM leads to endothelial cell dysfunction. (*A*) Confluent WT and $TM^{-/-}$ cells were fixed, permeabilized, and stained with rabbit anti-VE-cadherin antibody and Alexa Fluor 488–conjugated goat anti-rabbit IgG. F-actin was stained with Alexa Fluor 568–conjugated phalloidin followed by nucleus staining with Hoechst 33342. Immunofluorescence images were obtained with confocal microscopy. (Scale bar, 50 μm.) (*B*) Confluent WT and $TM^{-/-}$ cells were lysed, and levels of VE-cadherin (phosphorylated at Tyr658 and the total level), ZO-1, TM, and β-actin were analyzed by Western blotting. (*C*) Quantification (fold changes) in P-VE-cadherin (Y658) normalized to total VE-cadherin. Confluent WT and $TM^{-/-}$ cells were serum starved with basal medium containing 0.5% bovine serum albumin (BSA) for 3 h and then treated with either thrombin (1 nM) for 20 min (*D*) or TNF-α (10 ng/mL) for 4 h (*E*). The amount of Evans blue dye that leaked into the lower chamber in the Transwell assay plates was measured as described in *Materials and Methods*. (*F*) WT and $TM^{-/-}$ cells were treated with TNF-α (20 ng/mL) for various time points and levels of p65 NF-κB (phosphorylated and total); TM and β-actin were analyzed by Western blotting. (*G*) Cell surface levels of ICAM-1 in WT and $TM^{-/-}$ cells, treated with 1 and 10 ng/mL TNF-α for 4 h, were measured by flow cytometry. The untreated data belong to $TM^{-/-}$ cells. Data are mean ± SEM ($n = 3$). One-way ANOVA: $^{*}P < 0.05$, $^{**}P < 0.01$, and $^{***}P < 0.001$.

leading to increased endothelial cell permeability (13). Indeed, $TM^{-/-}$ cells exhibited increased basal permeability and hyperpermeability when stimulated with 1 nM thrombin (Fig. 1*D*). A similar barrier-disruptive effect was observed in $TM^{-/-}$ cells with electric impedance measurement by the xCELLigence system in response to thrombin (*SI Appendix*, Fig. S2*B*). Stimulation with TNF-α also resulted in a markedly higher permeability response in $TM^{-/-}$ cells (Fig. 1*E*). Additionally, TNF-α resulted in markedly higher p65 NF-κB phosphorylation in $TM^{-/-}$ cells (Fig. 1*F*). TNF-α also augmented the cell surface expression of intercellular adhesion molecule-1 (ICAM-1) (Fig. 1*G*) and vascular cell adhesion molecule-1 (VCAM-1) (*SI Appendix*, Fig. S2*C*) in $TM^{-/-}$ cells at a greater extent than wild-type cells. Taken together, these results suggest that TM plays a key role in maintaining a quiescence phenotype for endothelial cells under basal conditions and dampens the inflammatory function of cytokines under stimulated conditions.

**TM Plays a Modulatory Role in PAR1-Dependent Endothelial Cell Stimulation by Thrombin.** The activation of endothelial PAR1 by thrombin exhibits a concentration-dependent dual specificity with thrombin concentrations above 0.5 nM inducing a barrier-disruptive effect and a low concentration (i.e., 50 pM) eliciting a barrier-protective effect by unknown mechanisms (14, 15). In agreement with the literature, 1 nM thrombin induced a barrier-disruptive effect through cleavage of PAR1 in both wild-type and $TM^{-/-}$ cells since the PAR1 function-blocking antibody (ATAP2) blocked the thrombin effect on both cells (Fig. 2*A*). The nonblocking S-19 anti-PAR1 antibody was used as a control in these experiments. The protective effect of the low concentration of thrombin in endothelial cells was also PAR1 dependent; however, the protective effect of this low concentration of thrombin was eliminated in $TM^{-/-}$ cells (Fig. 2*B*). These results suggest that the PAR1-dependent barrier-protective activity of the low concentration of thrombin is mediated through the TM–thrombin complex, and the PAR1-dependent barrier-disruptive effect of the higher concentration of thrombin is largely due to free thrombin in the reaction. Analysis of cell surface expression levels of the EPCR and PAR1 in both wild-type and $TM^{-/-}$ cells indicated similar expression levels on both cell types (*SI Appendix*, Fig. S3 *A* and *B*).

**Reexpression of TM in $TM^{-/-}$ Cells Normalizes the Inflammatory Phenotype.** TM was reexpressed in $TM^{-/-}$ cells using lentivirus-mediated TM transduction, and cells expressing TM similar to that of wild-type cells ($TM^{match}$) were selected by the fluorescence-activated cell sorter (FACS) (*SI Appendix*, Fig. S3*C*). Immunostaining, Western blotting (*SI Appendix*, Fig. S3 *D* and *E*), and protein C activation levels by thrombin (data not shown) positively correlated with TM expression levels on $TM^{match}$ cells. Increased basal permeability and thrombin-induced hyperpermeability of $TM^{-/-}$ cells were attenuated in

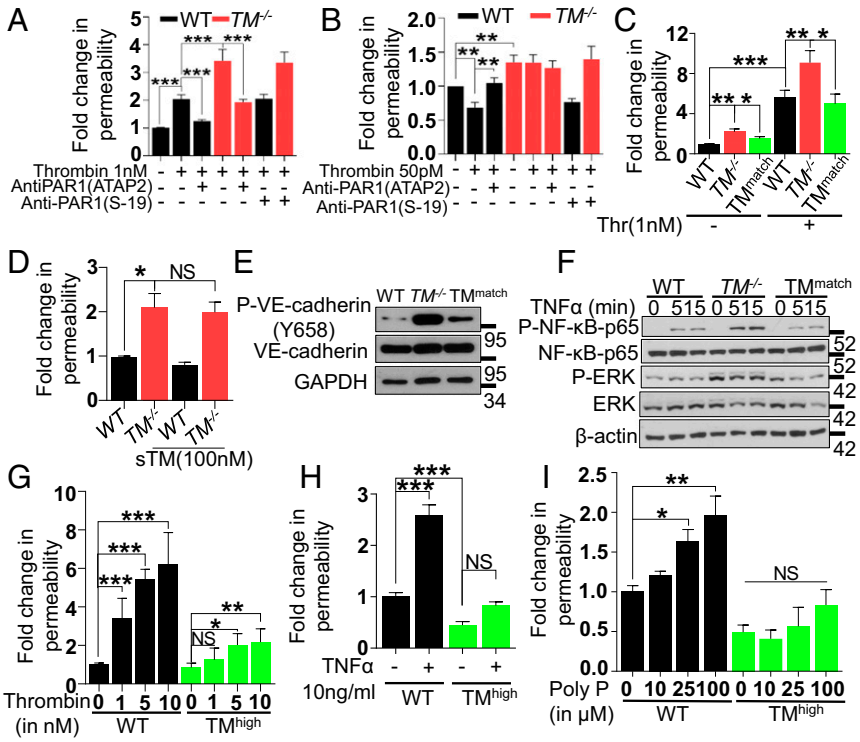


**Fig. 2.** Thrombin-mediated PAR1 signaling in $TM^{-/-}$ cells with or without lentivirus-mediated TM transduction. (*A*) Confluent WT and $TM^{-/-}$ cells were serum starved for 3 h before the addition of PAR1 function-blocking (ATAP2) or nonblocking (S19) antibodies for 30 min. Permeability was induced with thrombin (1 nM) for 20 min. The amount of Evans blue dye that leaked into the lower chamber in the Transwell assay plates was measured as described in *Materials and Methods*. (*B*) Confluent WT and $TM^{-/-}$ cells were pretreated with the same antibodies as in *A*, followed by treatment with thrombin (50 pM) in the basal medium containing 0.5% BSA for 3 h. The amount of Evans blue dye that leaked into the lower chamber in the Transwell assay plates was measured as described in *Materials and Methods*. (*C*) Similar to *A*, except in addition to WT and $TM^{-/-}$ cells, $TM^{match}$ cells were used. (*D*) Confluent WT, $TM^{-/-}$, and $TM^{match}$ cells were pretreated with sTM (100 nM) for 3 h before addition of Evans blue dye. (*E*) Confluent WT, $TM^{-/-}$, and $TM^{match}$ cells were lysed, and levels of VE-cadherin (phosphorylated at Tyr658 and the total), TM, and GAPDH were analyzed by Western blotting. (*F*) Confluent WT, $TM^{-/-}$, and $TM^{match}$ cells were treated with TNF-α (20 ng/mL) for 0, 5, and 15 min, and levels of p65 NF-κB (phosphorylated and total), ERK (phosphorylated and total), and β-actin were analyzed by Western blotting. (*G*) Confluent WT, $TM^{-/-}$, and $TM^{high}$ cells were serum starved with basal medium containing 0.5% BSA for 3 h and then treated with various concentrations of thrombin (1 to 10 nM) for 20 min, TNF-α (10 ng/mL) for 4 h (*H*), and polyphosphate (10-100 μM) for 4 h (*I*). The amount of Evans blue dye that leaked into the lower chamber in the Transwell assay plates was measured as described in *Materials and Methods*. Data are mean ± SEM ($n = 3$). One-way ANOVA: NS, non significant, $^*P < 0.05$, $^{**}P < 0.01$, and $^{***}P < 0.001$.

$TM^{match}$ cells (Fig. 2*C*). Unlike transduced TM, soluble TM (sTM) had no effect on restoring the basal permeability of $TM^{-/-}$ cells to a normal level (Fig. 2*D*), suggesting cell-bound TM is required for maintenance of normal vascular permeability. Moreover, the associated increased VE-cadherin phosphorylation was reduced in $TM^{match}$ cells (Fig. 2*E*). Similar results were obtained with TNF-α-mediated phosphorylation of p65 NF-κB in $TM^{match}$ cells (Fig. 2*F*). An increase in the basal phosphorylation of ERK in $TM^{-/-}$ cells was also observed (Fig. 2*F*). These inflammatory responses were all normalized in $TM^{match}$ cells. Taken together, these results suggest the loss of TM is responsible for the basal inflammatory phenotype of $TM^{-/-}$ cells. Cells expressing high levels of TM were also prepared by the lentivirus–TM construct ($TM^{high}$). Analysis of the barrier permeability function of $TM^{high}$ cells in response to increasing concentrations of thrombin indicated that 1 nM thrombin, which is sufficient to cleave all cell surface PAR1 on EA.hy926 cells and induce an inflammatory phenotype, did not induce a barrier-disruptive effect in these cells (Fig. 2*G*). The slight increase in the barrier permeability effect with higher concentrations of thrombin is likely due to the protease cleavage of PAR4 and/or other receptors. These results support our hypothesis that interaction of thrombin with TM abrogates its PAR1-dependent proinflammatory function. Interestingly, relative to wild-type cells, the basal permeability was markedly reduced in $TM^{high}$ cells (Fig. 2*H*), and the proinflammatory stimuli like TNF-α and polyphosphate, which are known to induce potent barrier-disruptive effects (16), were ineffective in $TM^{high}$ cells (Fig. 2 *H* and *I*).

**Leukocytes and Platelets Bind to $TM^{-/-}$ Endothelial Cells.** An increase in the cell surface expression of ICAM-1 was observed in $TM^{-/-}$ cells under unstimulated conditions, which were restored to normal levels in $TM^{match}$ cells (*SI Appendix*, Fig. S3*F*). Analysis of cell surface expression levels of ICAM-1 and E-selectin after stimulation with a low concentration of TNF-α (1 ng/mL) indicated that expression of both receptors is significantly enhanced in $TM^{-/-}$ cells but was restored to wild-type levels in $TM^{match}$ cells (Fig. 3 *A* and *B*). To determine the functional significance of enhanced expression levels of these receptors in $TM^{-/-}$ cells, an established adhesion assay under flow conditions was conducted by perfusing HL-60 cells on confluent monolayers of wild-type, $TM^{-/-}$, and $TM^{match}$ cells treated with a low concentration of TNF-α (1 ng/mL) in a flow chamber assay at 0.25 dyn/cm$^2$. $TM^{-/-}$ cells exhibited enhanced interaction with HL-60 cells (Fig. 3*C*). HL-60 cells rolled slowly before adhering firmly to $TM^{-/-}$ cells (Movie S2). A significant number of HL-60 cells also adhered to nonstimulated $TM^{-/-}$ cells. However, wild-type and $TM^{match}$ cells exhibited an insignificant level of adhesion to HL-60 cells under both stimulated and nonstimulated conditions (Fig. 3*C* and Movies S1 and S3). The flow chamber assay was also employed to monitor adhesion of freshly isolated platelets to endothelial cells with or without stimulation of cells with a low concentration of HMGB1 (20 nM), which does not induce any change in VWF levels in wild-type cells (*SI Appendix*, Fig. S4*A*). An increased number of platelet string formations was observed only on $TM^{-/-}$ cells, the extent of which was significantly higher on HMGB1-stimulated cells (Fig. 3 *D* and *E* and Movie S5). By contrast, minimal platelet–endothelial cell interaction was observed in wild-type and $TM^{match}$ cells, with or without HMGB1 stimulation (Fig. 3 *D* and *E* and Movies S4 and S6).

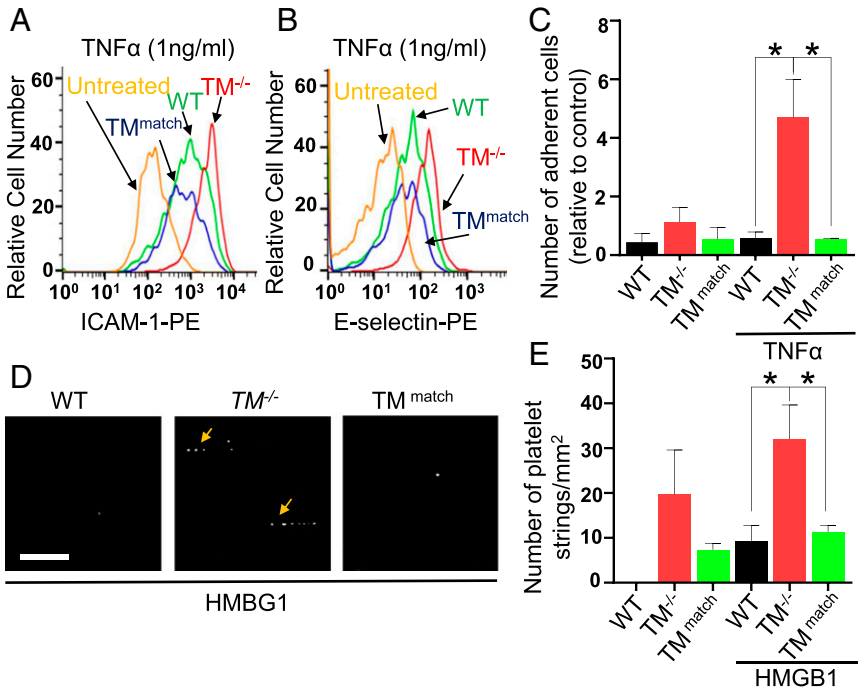


**Fig. 3.** Lentivirus-mediated reexpression of TM in $TM^{-/-}$ cells inhibits TNF-α-induced adhesion of HL-60 cells and HMBG1-induced platelet string formation on $TM^{-/-}$ cells. (*A*) Cell surface levels of ICAM-1 and (*B*) E-selectin in WT, $TM^{-/-}$, and $TM^{match}$ cells, treated with TNF-α (1 ng/mL) for 4 h, were measured by flow cytometry. $TM^{-/-}$ cells were used as untreated controls. (*C*) Fold change in the adhesion of HL-60 cells on WT, $TM^{-/-}$, and $TM^{match}$ cells, stimulated with TNF-α (1 ng/mL) for 4 h under flow conditions per field of the view (firmly adherent cells were quantified). (*D*) WT, $TM^{-/-}$, and $TM^{match}$ cells were incubated with HMGB1 (20 nM) for 18 h and then 5-chloromethylfluorescein diacetate–labeled platelets were perfused in a flow chamber. Representative images showing platelet string formation captured on WT, $TM^{-/-}$, and $TM^{match}$ cells. (Scale bar, 25μm.) (*E*) Quantitation was measured by counting the average number and length of strings per field in different groups. The average number of platelet strings per field was determined as ≥3 platelets aligned in the direction of the flow. Data are mean ± SEM ($n$ = 3). One-way ANOVA: *$P$ < 0.05.

**Increased VWF Expression and Release Are Responsible for Platelet String Formation in $TM^{-/-}$ Cells.** Platelet string formation occurs on endothelial cells only upon release of high-molecular-weight VWF molecules (17, 18). Increased platelet–endothelial interactions prompted us to determine whether $TM^{-/-}$ cells constitutively secrete or synthesize VWF that resulted in increased platelet string formation. Hence, supernatants from both WT and $TM^{-/-}$ cells were collected and analyzed for VWF secretion by enzyme-linked immunosorbent assay (ELISA). Surprisingly, there was a dramatic increase in the basal level of VWF release from $TM^{-/-}$ cells compared to WT cells (Fig. 4*A*). Increased VWF release was also detected in supernatants of the heterozygous $TM^{+/-}$ cells, the extent of which was almost half of that observed with the homozygous $TM^{-/-}$ cell (Fig. 4*A*). Analysis of VWF particles in wild-type and $TM^{-/-}$ cells by confocal imaging revealed an increased stochastic expression of VWF in $TM^{-/-}$ cells (*SI Appendix*, Fig. S4*B*). Furthermore, analysis of a single cell at a higher magnification and a subsequent three-dimensional surface plot of VWF particles in the cell cytoplasm indicated a uniform distribution and thickness for VWF particles in wild-type cells but an increase in both the number and size of the VWF particles in $TM^{-/-}$ cells (Fig. 4*B*). Results of Western blotting and real-time RT-PCR indicated that TM deficiency increases both protein (Fig. 4 *C* and *D*) and messenger ribonucleic acid (mRNA) transcript levels of VWF (Fig. 4*E*).

Angiopoietin-2 (Ang2) is another regulatory molecule that is localized with VWF in Weibel–Palade bodies (WPBs) and released upon activation of endothelial cells by various physiological stimuli (19, 20). Since a direct interaction between TM and Ang2 has been reported (21), we decided to evaluate Ang2 expression in $TM^{-/-}$ cells. Intriguingly, there was a marked decrease in Ang2 secretion in $TM^{+/-}$ and $TM^{-/-}$ cells as determined by ELISA (Fig. 4*F*). Western blotting results further confirmed the decreased expression of Ang2 in $TM^{-/-}$ cells (Fig. 4*G*). Both thrombin and TNF-α are known to increase expression level and the release of Ang2 from WPBs (22). However, stimulation of cells with either thrombin (10 nM) or TNF-α (100 ng/mL) did not induce a significant amount of Ang2 release in $TM^{-/-}$ cells when compared to wild-type cells (Fig. 4*H*). Confocal imaging indicated a low Ang2 level in the cytoplasm of $TM^{-/-}$ cells (*SI Appendix*, Fig. S4*C*), suggesting increased expression and storage of VWF limits the synthesis and/or the storage of Ang2 in WPBs of $TM^{-/-}$ cells. These results are consistent with the literature since expression levels of VWF and Ang2 are known to be inversely related and an enhanced VWF expression level is associated with inhibition of Ang2 expression in vascular endothelial cells (20).

**Reexpression of TM in $TM^{-/-}$ Cells Normalizes VWF and Ang2 Levels.** Reexpression of TM attenuated expression of VWF mRNA and reversed decreased the Ang2 mRNA expression level in $TM^{match}$



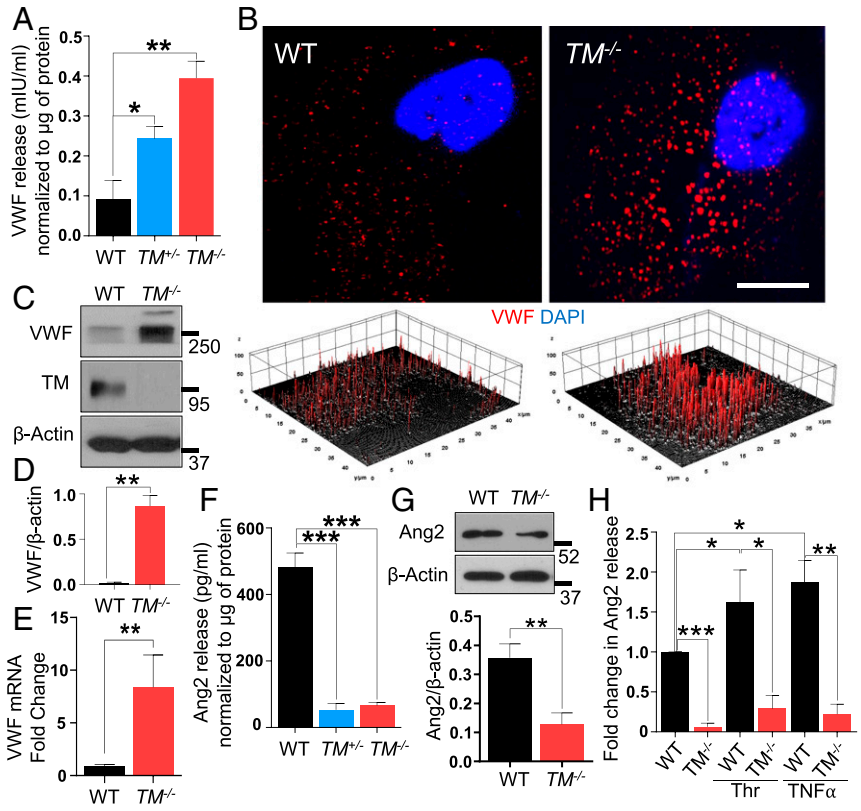


**Fig. 4.** Deficiency of TM leads to increased expression and release of VWF. (*A*) Levels of VWF in the medium supernatant collected from confluent WT, $TM^{+/-}$, and $TM^{-/-}$ cells were measured by a sandwich ELISA. (*B*) Confluent WT and $TM^{-/-}$ cells were fixed, permeabilized, and stained with rabbit anti-VWF antibody and Alexa Fluor 568–conjugated goat anti-rabbit IgG. The nucleus was stained with Hoechst 33342. Immunofluorescence images were obtained with confocal microscopy. A three-dimensional surface plot of VWF particles in the cytoplasm, constructed with ImageJ software, is presented below *B*. (Scale bar, 10 µm.) (*C*) Confluent WT and $TM^{-/-}$ cells were lysed, and protein levels of VWF, TM, and β-actin were analyzed by Western blotting. (*D*) Quantitation of VWF protein levels inside the cells normalized to β-actin. (*E*) Changes in VWF RNA transcripts in WT and $TM^{-/-}$ cells were measured by qRT-PCR. GAPDH was used as an internal control for quantitation. (*F*) Levels of Ang2 in the medium supernatant, collected from the same cells mentioned in *A*. (*G*) Protein levels of Ang2 and β-actin in confluent WT and $TM^{-/-}$ cells were measured by Western blotting along with the quantitation. (*H*) Levels of Ang2 in the medium supernatant, collected from confluent WT and $TM^{-/-}$ cells, treated with thrombin (10 nM) or TNF-α (100 ng/mL) for 16 h, were measured by a sandwich ELISA. Data are mean ± SEM ($n = 3$). One-way ANOVA: $^{*}P < 0.05$, $^{**}P < 0.01$, and $^{***}P < 0.001$.

cells as determined by RT-PCR (Fig. 5*A*). Similar results were obtained at the protein level; thus, a reduction in the protein level of VWF in TM$^{match}$ cells was accompanied by an increase in the expression level of Ang2 (Fig. 5 *B–D*). Analysis of VWF and Ang2 protein levels in supernatants by ELISA further confirmed that reexpression of TM is associated with restoration of normal expression of VWF (Fig. 5*E*) and Ang2 (Fig. 5*F*) in TM$^{match}$ cells (Fig. 5*F*). Interestingly, TM$^{high}$ cells showed decreased basal levels of VWF release in the supernatant as well as protein levels in the cell lysate (Fig. 5 *G* and *H*).

Soluble TM has been known to exhibit anti-inflammatory effects in endothelial cells (7). To determine whether the signaling function of sTM, similar to reexpression of TM, can normalize the expression level of VWF in $TM^{-/-}$ cells, cells were treated with sTM for 16 h before measuring VWF release in wild-type and $TM^{-/-}$ cells. Analysis by ELISA revealed sTM has no effect on VWF release (Fig. 5*I*), suggesting that cell-bound TM is required for regulation of expression and storage of VWF in WPBs. To determine whether increased VWF in $TM^{-/-}$ cells is responsible for the increased basal barrier permeability, short hairpin ribonucleic acid (shRNA) was used to knock down VWF in $TM^{-/-}$ cells (*SI Appendix*, Fig. S5*A*). The results showed VWF knockdown could not restore basal cell permeability similar to that seen in TM$^{match}$ cells (*SI Appendix*, Fig. S5*B*).

**Inflammation and Increased VWF Expression in the Lungs of TM Knockout Mice.** Next, we investigated the expression profile of VWF in tamoxifen-treated ERcre-$TM^{f/f}$ (TM-KO) mice. Whole-mount immunostaining of the mouse trachea at day 12 of tamoxifen treatment showed ~90% deletion of TM (Fig. 6 *A* and *B*). Results indicated expression of VWF in venular endothelial cells was markedly increased (Fig. 6 *A* and *C*). Analysis of the lung lysates revealed tamoxifen treatment markedly decreased TM levels in TM-KO mice, and the VWF expression level was also significantly elevated in these mice (Fig. 6 *D* and *E*). Increased VWF and decreased TM antigen levels in the lung lysates were further confirmed by ELISA in TM-KO mice in comparison to $TM^{f/f}$ (Fig. 6 *F* and *G*). Microscopic examination of the paraffin-embedded sections of lung tissues stained with hematoxylin and eosin (H&E) displayed increased inflammatory foci in the lungs (Fig. 6*H*), reminiscent of the increased basal inflammatory phenotype of $TM^{-/-}$ cells.

A slight but statistically nonsignificant increase in the plasma level of VWF was observed in TM-KO mice (*SI Appendix*, Fig. S6*A*). However, the plasma level of Ang2 was significantly reduced in TM-KO mice (*SI Appendix*, Fig. S6*B*), suggesting increased VWF expression is also associated with reduced Ang2 levels in vivo similar to that seen in $TM^{-/-}$ cells in vitro. Multimer analysis of VWF derived from cell culture supernatants and mice are shown in *SI Appendix*, Fig. S7 *A* and *B*. No changes in the plasma clotting time and activated partial thromboplastin time were observed among $TM^{f/f}$ and TM-KO mice (*SI Appendix*, Fig. S6 *C* and *D*), suggesting increased VWF expression is not as a result of activation of blood coagulation but due to the loss of TM from endothelial cells. Taken together, these results suggest that cell-bound TM plays a key role in regulation of the basal permeability function of endothelial cells, thereby contributing to both the maintenance of the quiescence phenotype of blood vessels under normal conditions and down-regulation of inflammatory responses under stimulated conditions (model in Fig. 7).

## Discussion

Both primary and transformed HUVECs are extensively used for investigating mechanistic details of PAR1 signaling by thrombin and other coagulation proteases in vascular endothelial cells. In addition to PAR1, these cells express at least three other receptors: PAR3, PAR4, and TM, which are also targets for interaction with thrombin. With the exception of PAR4, the other three receptors (PAR1, PAR3, and TM) all possess a hirudin-like sequence that binds to exosite-1 of thrombin to modulate the procoagulant and signaling specificity of the protease (10, 23,

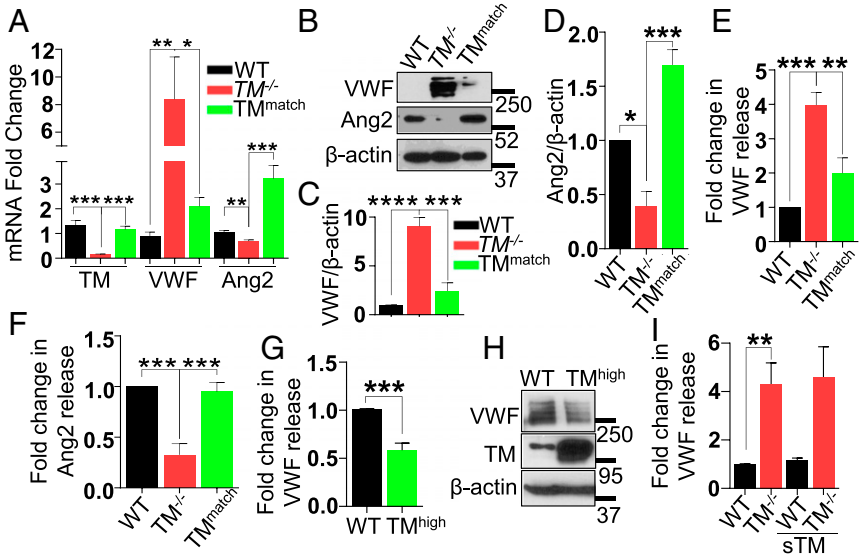


**Fig. 5.** Lentivirus-mediated reexpression of TM in $TM^{-/-}$ cells, but not sTM, normalizes VWF and Ang2 levels. (*A*) Levels of VWF, Ang2, and TM RNA transcripts in WT, $TM^{-/-}$, and TM$^{match}$ were measured by qRT-PCR. GAPDH was used as an internal control for quantitation. (*B*) Confluent WT, $TM^{-/-}$, and TM$^{match}$ cells were lysed, and levels of VWF, Ang2, and β-actin were analyzed by Western blotting. Quantitation of changes in the levels of (*C*) VWF and (*D*) Ang2 in WT, $TM^{-/-}$, and TM$^{match}$ cells. Levels of (*E*) VWF and (*F*) Ang2 in the medium supernatant collected from confluent WT, $TM^{-/-}$, and TM$^{match}$ cells. (*G*) Levels of VWF in the medium supernatant collected from confluent WT and TM$^{high}$ cells were measured by a sandwich ELISA. (*H*) Confluent WT and TM$^{high}$ cells were lysed, and levels of VWF, TM, and β-actin were analyzed by Western blotting. (*I*) Confluent WT and $TM^{-/-}$ cells were treated with sTM (100 nM) for 16 h in the basal medium containing 0.5% BSA, and levels of VWF in the medium supernatant were analyzed by a sandwich ELISA. Data are mean ± SEM ($n = 3$). One-way ANOVA: *$P < 0.05$, **$P < 0.01$, ***$P < 0.001$, and ****$P < 0.001$.

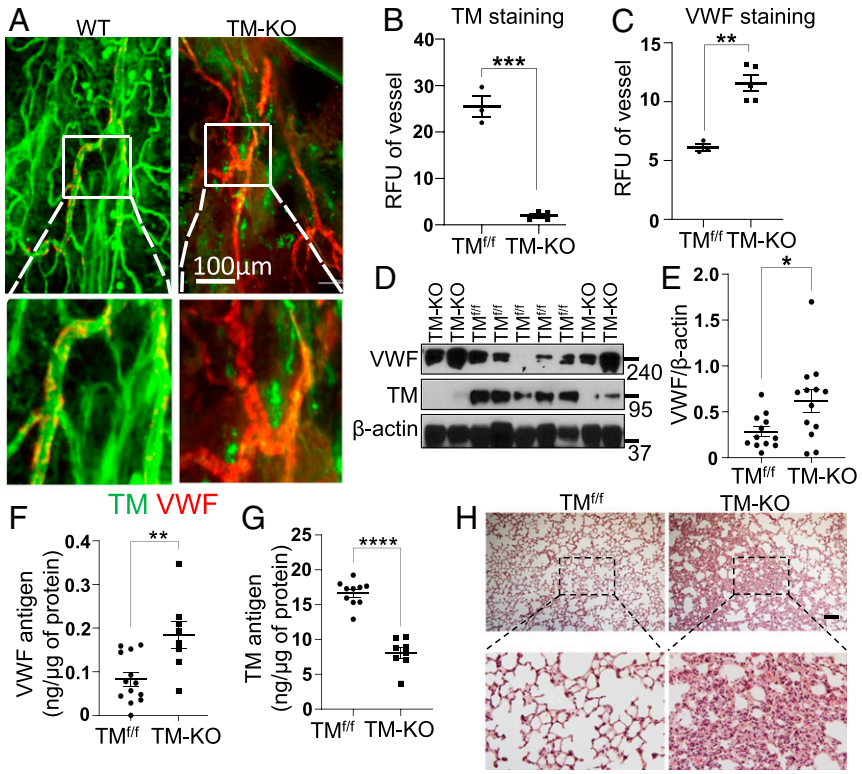


**Fig. 6.** Increased expression of VWF in the trachea vessels and lungs in TM-KO mice. (*A*) Tracheal blood vessels visualized by TM and VWF immunostaining of $TM^{f/f}$ and TM-KO mice. The inset boxes from each group are magnified. Note the prominent expression of VWF in veins (shown in the inset box). (Scale bar, 100 μm.) (*B* and *C*) Relative fluorescence intensity units (RFU) of TM and VWF in tracheal vessels analyzed by ImageJ in $TM^{f/f}$ ($n = 3$) and TM-KO ($n = 5$) mice. (*D*) Lung lysates from $TM^{f/f}$ and TM-KO mice were analyzed for protein levels of TM, β-actin, and VWF by Western blotting. (*E*) Quantitation of VWF normalized to β-actin in WT ($n = 12$) and TM-KO ($n = 13$) mice. (*F*) Tissue antigen levels of VWF in $TM^{f/f}$ ($n = 13$) and TM-KO ($n = 8$) mice measured by a sandwich ELISA. (*G*) TM antigen levels in the lung lysates of $TM^{f/f}$ ($n = 10$) and TM-KO ($n = 8$) mice were measured by a sandwich ELISA. (*H*) Representative images (10×) of H&E staining of the lung tissue sections from $TM^{f/f}$ and TM-KO mice. The inset boxes from each group are magnified. (Scale bar, 200 μm.) Data are mean ± SEM ($n = 3$). *t* test: $^*P < 0.05$, $^{**}P < 0.01$, $^{***}P < 0.001$, and $^{****}P < 0.001$.

24). PAR3 does not have a cytoplasmic domain, and thus, this receptor is not believed to be directly involved in signaling by thrombin. However, thrombin cleavage of both PAR1 and PAR4 induces barrier-disruptive effects in cultured endothelial cells (5, 25, 26). Thrombin exhibits a dual PAR1 signaling specificity with concentrations in the picomolar range (50 pM), inducing a barrier-protective effect, however, in the nanomolar range (>1 nM), eliciting a barrier-disruptive effect (14, 15). To evaluate the contribution of TM to the signaling specificity of thrombin in this system, we deleted the TM gene from EA.hy926 cells and studied the PAR1-dependent signaling function of thrombin in $TM^{-/-}$ cells. Interestingly, we found that the PAR1-dependent barrier-disruptive function of thrombin (1 nM) in $TM^{-/-}$ cells was markedly enhanced. However, further studies revealed that the fold enhancement in the barrier-disruptive function of thrombin is similar for both wild-type and $TM^{-/-}$ cells and that the enhanced effect in $TM^{-/-}$ cells was primarily due to markedly compromised basal permeability, suggesting TM plays a key role in the maintenance of a noninflammatory phenotype for endothelial cells under normal conditions. In support of this hypothesis, the impaired basal permeability was rescued in $TM^{-/-}$ cells if they were transduced with a TM–lentivirus construct. Interestingly, analysis of results of permeability assays indicated that the PAR1-dependent barrier-protective effect of the low concentration of thrombin is absent in $TM^{-/-}$ cells, strongly suggesting this effect of thrombin is dependent on binding of the protease to TM on endothelial cells. It appears that the cell surface expression level of TM on EA.hy926 cells is rather low; thus, most of the added thrombin (1 nM) remains unbound under these assay conditions. The finding that the TM–thrombin complex induces a barrier-protective effect is significant as it implies that the PAR1-dependent signaling specificity of thrombin would be of the barrier-protective type in the microvasculature where the surface area of the endothelium, exposed per milliliter of blood, is dramatically increased and thus the effective local concentration of TM can reach a very high level (~500 nM) (27–29). Further support for the hypothesis that interaction with TM abrogates the PAR1-dependent proinflammatory function of thrombin is provided by the observation that unlike wild-type and $TM^{match}$ cells, $TM^{high}$ cells, which express ~10-fold higher TM levels, exhibited resistance to the barrier-disruptive effect of high concentrations of thrombin and other proinflammatory stimuli (Fig. 2), suggesting a key role for the cell-bound TM in conferring high stability for endothelial cell junctions.

The increased basal permeability of $TM^{-/-}$ cells was associated with decreased polymerization of cortical actin microfilaments and phosphorylation-dependent destabilization of VE-cadherin at cellular adherens junctions (Fig. 1). Cortical actin microfilaments are attached to transmembrane proteins, and they play crucial roles in the maintenance of the endothelial barrier function and cell shape as their disruption by cytochalasin B has been shown to lead in increased endothelial cell permeability (30). The results of this study suggest the membrane-bound TM may be part of other transmembrane proteins that are involved in the maintenance of the integrity of cortical actin

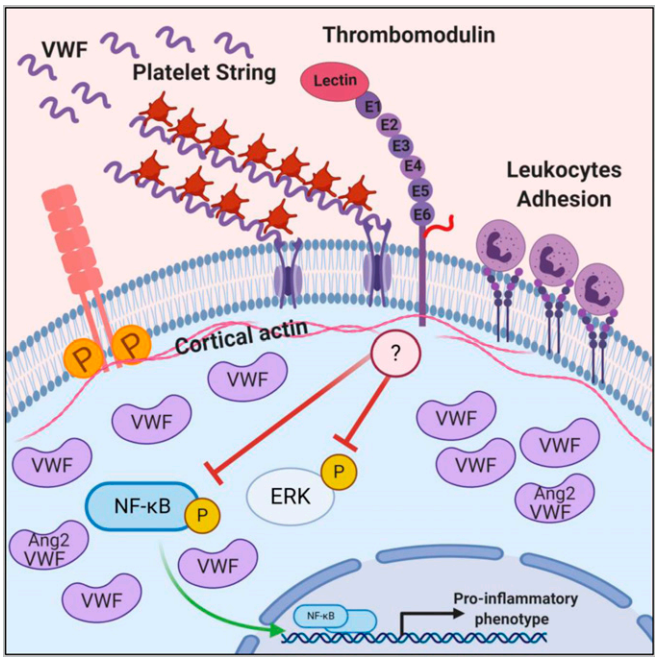


**Fig. 7.** Schematic illustration showing that deletion of TM results in NF-κB and ERK phosphorylation, increased endothelial permeability, phosphorylation of VE-cadherin, loss of cortical actin, increased expression of inflammatory adhesion molecules, increased adhesion of leukocytes, and platelet string formation. Altered WPB content (increased expression, storage, and release of VWF and decreased expression, storage, and release of Ang2) is denoted. Image was created with BioRender.

microfilaments and the cell shape. The soluble form of TM did not rescue the impaired basal permeability function of $TM^{-/-}$ cells; however, reexpression of full-length TM restored it to a normal level (Fig. 2). Moreover, relative to wild-type cells, the basal permeability was significantly improved in $TM^{high}$ cells, suggesting the cell-bound TM plays a key role in stabilizing the interaction of actin microfilaments with VE-cadherin and other transmembrane proteins at the cellular junctions. The mechanism by which TM interacts with cytoskeletal membrane proteins to regulate basal permeability is not known. It is, however, known that TM interacts directly with the actin cytoskeleton by membrane-anchoring proteins called ERM proteins, which are involved in controlling cell shape by attaching cortical actin microfilaments to the cell membrane. A direct interaction between TM and ezrin (31), one of the three closely related proteins of ERM (ezrin, radixin, and moesin), has been reported. Further support for our hypothesis is provided by results of a previous study which showed that the cytoplasmic domain–dependent signaling function of TM is required for its antiproliferative function (32). It should also be noted that in addition to compromised basal permeability, the basal expression levels of cell adhesion molecules were elevated in $TM^{-/-}$ cells and these cells were also hyperresponsive when stimulated with cytokines. Further studies are required to understand the exact mechanism by which TM contributes to the regulation of vascular permeability and maintenance of the quiescence phenotype in endothelial cells.

Another interesting observation of this study is the dramatically increased expression and secretion levels of VWF in $TM^{-/-}$ cells under basal conditions (Fig. 4). Thrombin and other inflammatory stimuli are known to activate endothelial cells and mobilize VWF to the cell surface, thereby recruiting platelets and forming long string-like structures that play critical roles in regulating primary hemostasis at the vascular injury site. A significant fraction of the released VWF appears to remain attached to the surface of $TM^{-/-}$ cells as evidenced by their ability to recruit freshly isolated platelets and form the characteristic cell surface platelet strings in a flow chamber assay (Fig. 3). The markedly enhanced release of VWF in unstimulated $TM^{-/-}$ cells suggests that apart from its essential anticoagulant role in promoting protein C activation by thrombin, TM also plays a critical anticoagulant and anti-inflammatory role by regulating the VWF release from WPBs. This finding may have clinical relevance in inflammatory disorders where expression of TM is downregulated during inflammation and/or the receptor is cleaved by metalloproteases and leukocyte proteases and released to the circulation as soluble TM (33, 34). Similar to VWF-mediated adhesion to platelets, the increased basal expression of CAMs on $TM^{-/-}$ cells promoted adhesion of HL-60 leukocytes to the cell surface. Whether decreased surface expression or cleavage of TM can increase secretion of VWF and expression of CAMs under inflammatory conditions requires further investigation.

In addition to VWF, another WPB protein, Ang2, which is colocalized with VWF in WPBs and released only upon stimulation, was also altered in $TM^{-/-}$ cells; in this case however, the secretion of Ang2 was markedly decreased (Fig. 4). Lentiviral-mediated TM transduction normalized expression of both VWF and Ang2 in $TM^{-/-}$ cells, supporting the hypothesis that TM is involved directly or indirectly in regulating expression, secretion, and storage of these proteins. Ang2 functions as an antagonist of Ang1-Tie2 signaling and acts synergistically with VEGF-A to promote angiogenesis (19, 20). Recent results have indicated that small interfering ribonucleic acid (siRNA) knockdown of VWF expression increases Ang2 release (20), suggesting that VWF negatively regulates angiogenesis. Consistent with these previous results, the enhanced expression of VWF culminated in inhibition of expression of Ang2 in $TM^{-/-}$ cells. The TM-dependent regulation of both angiogenic proteins was mediated at the transcriptional level since a markedly elevated VWF mRNA level in $TM^{-/-}$ cells was associated with a significant decrease in the mRNA expression level of Ang2. TM itself has also been shown to directly regulate angiogenesis. The EGF-like domain of TM promotes angiogenesis (35); however, the lectin-like domain of TM has been reported to inhibit angiogenesis through interaction with the Lewis Y antigen on endothelial cells (36). The observation that sTM did not restore the expression levels of either VWF or Ang2 in $TM^{-/-}$ cells suggests that signaling by the lectin-like domain of TM may not be involved in TM-dependent paradoxical regulation of VWF and Ang2 as observed in this study. Based on the observation that deletion of the TM gene leads to destabilization of VE-cadherin and cortical actin filaments, we favor the hypothesis that TM is associated with other transmembrane proteins which are involved in regulation of vascular tone and angiogenesis. The integrin αvβ3 has been identified as the primary receptor for VWF on endothelial cells (20). In light of reports that Ang2 also interacts with αvβ3 to regulate angiogenesis, further studies will be required to determine whether αvβ3 is one of the transmembrane protein network that is also directly or indirectly associated with TM in endothelial cells.

Finally, analysis of the expression profile of VWF in trachea and lung lysates in TM-KO mice indicates that the findings in the cellular system are physiologically relevant. Immunostaining of the mouse trachea clearly indicated that expression of VWF in venular endothelial cells was markedly increased in TM-KO mice. Although the increase in the plasma level of VWF was not statistically significant on day 12 of the experiment, TM deficiency was associated with a significant increase of VWF expression in endothelial cells and reduction in the plasma level of Ang2 in TM-KO mice, supporting the findings in the cellular model. As expected, increased inflammatory foci in the lungs of TM-KO animals were also observed, which is reminiscent of the

increased basal inflammatory phenotype of $TM^{-/-}$ cells. Further studies in cellular and animal models in which the cytoplasmic domain of TM has been deleted are required to further investigate the hypothesis that the interaction of cell-bound TM with transmembrane or cytoskeletal proteins plays a key role in maintaining the vascular integrity and basal quiescence phenotype of endothelial cells.

## Materials and Methods

All protocols were approved by the Institutional Review Board and Use Committee of the Oklahoma Medical Research Foundation. Blood was collected in acid–citrate–dextrose tubes from healthy adult volunteers with informed consent. Reagents, cell culture methods, generation of $TM^{-/-}$ cells, lentivirus-based overexpression of TM, knockdown of VWF in $TM^{-/-}$ cells, TM knockout mouse model, ELISA, VWF–platelet string formation assay, endothelial cell permeability assay, cell index measurement, immunofluorescence microscopy, whole-mount immunostaining of trachea, sodium dodecyl sulphate–polyacrylamide gel electrophoresis (SDS-PAGE) and Western blotting, RNA isolation and qRT-PCR analysis, flow cytometry, cell adhesion assays under flow conditions, histological analysis, protein C activation assay by thrombin, and statistical analysis are all described in *SI Appendix*.

**Data Availability.** All study data are included in the article and/or supporting information.

**ACKNOWLEDGMENTS.** We thank Cindy Carter for technical assistance, Huiping Shi for VWF multimer gel analysis, and Audrey Rezaie for editorial work on the manuscript. This work was supported by grants awarded by National Heart, Lung, and Blood Institute of NIH Grants HL101917 and HL62565 (to A.R.R.) and HL117132 (to H.W.).

1. C. T. Esmon, Thrombomodulin as a model of molecular mechanisms that modulate protease specificity and function at the vessel surface. *FASEB J.* **9**, 946–955 (1995).
2. B. Dahlbäck, B. O. Villoutreix, Regulation of blood coagulation by the protein C anticoagulant pathway: Novel insights into structure-function relationships and molecular recognition. *Arterioscler. Thromb. Vasc. Biol.* **25**, 1311–1320 (2005).
3. M. Riewald, R. J. Petrovan, A. Donner, B. M. Mueller, W. Ruf, Activation of endothelial cell protease activated receptor 1 by the protein C pathway. *Science* **296**, 1880–1882 (2002).
4. L. O. Mosnier, B. V. Zlokovic, J. H. Griffin, The cytoprotective protein C pathway. *Blood* **109**, 3161–3172 (2007).
5. A. R. Rezaie, Protease-activated receptor signalling by coagulation proteases in endothelial cells. *Thromb. Haemost.* **112**, 876–882 (2014).
6. H. Weiler, B. H. Isermann, Thrombomodulin. *J. Thromb. Haemost.* **1**, 1515–1524 (2003).
7. E. M. Conway *et al*., The lectin-like domain of thrombomodulin confers protection from neutrophil-mediated tissue damage by suppressing adhesion molecule expression via nuclear factor kappaB and mitogen-activated protein kinase pathways. *J. Exp. Med.* **196**, 565–577 (2002).
8. T. Ito, I. Maruyama, Thrombomodulin: Protectorate god of the vasculature in thrombosis and inflammation. *J. Thromb. Haemost.* **9**, 168–173 (2011).
9. T. E. van Mens *et al*., Variable phenotypic penetrance of thrombosis in adult mice after tissue-selective and temporally controlled Thbd gene inactivation. *Blood Adv.* **1**, 1148–1158 (2017).
10. L. W. Liu, T. K. Vu, C. T. Esmon, S. R. Coughlin, The region of the thrombin receptor resembling hirudin binds to thrombin and alters enzyme specificity. *J. Biol. Chem.* **266**, 16977–16980 (1991).
11. J. S. Bae, L. Yang, C. Manithody, A. R. Rezaie, The ligand occupancy of endothelial protein C receptor switches the protease-activated receptor 1-dependent signaling specificity of thrombin from a permeability-enhancing to a barrier-protective response in endothelial cells. *Blood* **110**, 3909–3916 (2007).
12. R. V. Roy, A. Ardeshirylajimi, P. Dinarvand, L. Yang, A. R. Rezaie, Occupancy of human EPCR by protein C induces β-arrestin-2 biased PAR1 signaling by both APC and thrombin. *Blood* **128**, 1884–1893 (2016).
13. P. Belvitch, Y. M. Htwe, M. E. Brown, S. Dudek, Cortical actin dynamics in endothelial permeability. *Curr. Top. Membr.* **82**, 141–195 (2018).
14. J. S. Bae, Y. U. Kim, M. K. Park, A. R. Rezaie, Concentration dependent dual effect of thrombin in endothelial cells via Par-1 and Pi3 kinase. *J. Cell. Physiol.* **219**, 744–751 (2009).
15. C. Feistritzer, M. Riewald, Endothelial barrier protection by activated protein C through PAR1-dependent sphingosine 1-phosphate receptor-1 crossactivation. *Blood* **105**, 3178–3184 (2005).
16. P. Dinarvand *et al*., Polyphosphate amplifies proinflammatory responses of nuclear proteins through interaction with receptor for advanced glycation end products and P2Y1 purinergic receptor. *Blood* **123**, 935–945 (2014).
17. Z. Zhou, J. F. Dong, Thrombotic thrombocytopenic purpura and anti-thrombotic therapy targeted to von Willebrand factor. *Curr. Vasc. Pharmacol.* **10**, 762–766 (2012).
18. K. M. Valentijn, J. E. Sadler, J. A. Valentijn, J. Voorberg, J. Eikenboom, Functional architecture of Weibel-Palade bodies. *Blood* **117**, 5033–5043 (2011).
19. M. G. Rondaij, R. Bierings, A. Kragt, J. A. van Mourik, J. Voorberg, Dynamics and plasticity of Weibel-Palade bodies in endothelial cells. *Arterioscler. Thromb. Vasc. Biol.* **26**, 1002–1007 (2006).
20. R. D. Starke *et al*., Endothelial von Willebrand factor regulates angiogenesis. *Blood* **117**, 1071–1080 (2011).
21. C. Daly *et al*., Angiopoietins bind thrombomodulin and inhibit its function as a thrombin cofactor. *Sci. Rep.* **8**, 505 (2018).
22. I. Kim, J. H. Kim, Y. S. Ryu, M. Liu, G. Y. Koh, Tumor necrosis factor-alpha upregulates angiopoietin-2 in human umbilical vein endothelial cells. *Biochem. Biophys. Res. Commun.* **269**, 361–365 (2000).
23. M. V. Malovichko, T. M. Sabo, M. C. Maurer, Ligand binding to anion-binding exosites regulates conformational properties of thrombin. *J. Biol. Chem.* **288**, 8667–8678 (2013).
24. M. Nakanishi-Matsui *et al*., PAR3 is a cofactor for PAR4 activation by thrombin. *Nature* **404**, 609–613 (2000).
25. J. S. Bae, A. R. Rezaie, Protease activated receptor 1 (PAR-1) activation by thrombin is protective in human pulmonary artery endothelial cells if endothelial protein C receptor is occupied by its natural ligand. *Thromb. Haemost.* **100**, 101–109 (2008).
26. S. R. Coughlin, Protease-activated receptors in hemostasis, thrombosis and vascular biology. *J. Thromb. Haemost.* **3**, 1800–1814 (2005).
27. C. Busch, P. A. Cancilla, L. E. DeBault, J. C. Goldsmith, W. G. Owen, Use of endothelium cultured on microcarriers as a model for the microcirculation. *Lab. Invest.* **47**, 498–504 (1982).
28. C. T. Esmon, Cell mediated events that control blood coagulation and vascular injury. *Annu. Rev. Cell Biol.* **9**, 1–26 (1993).
29. V. A. Ford, C. Stringer, S. J. Kennel, Thrombomodulin is preferentially expressed in Balb/c lung microvessels. *J. Biol. Chem.* **267**, 5446–5450 (1992).
30. N. Prasain, T. Stevens, The actin cytoskeleton in endothelial cell phenotypes. *Microvasc. Res.* **77**, 53–63 (2009).
31. Y. Y. Hsu *et al*., Thrombomodulin is an ezrin-interacting protein that controls epithelial morphology and promotes collective cell migration. *FASEB J.* **26**, 3440–3452 (2012).
32. Y. Zhang *et al*., Thrombomodulin modulates growth of tumor cells independent of its anticoagulant activity. *J. Clin. Invest.* **101**, 1301–1309 (1998).
33. Y. Jourdy *et al*., Why patients with THBD c.1611C>A (p.Cys537X) nonsense mutation have high levels of soluble thrombomodulin? *PLoS One* **12**, e0188213 (2017).
34. M. Menschikowski, A. Hagelgans, G. Eisenhofer, O. Tiebel, G. Siegert, Reducing agents induce thrombomodulin shedding in human endothelial cells. *Thromb. Res.* **126**, e88–e93 (2010).
35. C. S. Shi *et al*., Evidence of human thrombomodulin domain as a novel angiogenic factor. *Circulation* **111**, 1627–1636 (2005).
36. C. H. Kuo *et al*., The recombinant lectin-like domain of thrombomodulin inhibits angiogenesis through interaction with Lewis Y antigen. *Blood* **119**, 1302–1313 (2012).